Chemistry & Biology
Article

In Vivo Fluorescent Detection of Fe-S Clusters Coordinated by Human GRX2

Kevin G. Hoff,[1,2,4,*] Stephanie J. Culler,[1,4] Peter Q. Nguyen,[2] Ryan M. McGuire,[3] Jonathan J. Silberg,[2,3,*] and Christina D. Smolke[1]
[1]Division of Chemistry and Chemical Engineering, California Institute of Technology, 1200 E. California Boulevard, Mail Code 210-41, Pasadena, CA 91125, USA
[2]Department of Biochemistry and Cell Biology
[3]Department of Bioengineering
Rice University, 6100 Main Street, MS 140, Houston, TX 77005, USA
[4]These authors contributed equally to this work
*Correspondence: khoff@caltech.edu (K.G.H.), joff@rice.edu (J.J.S.)
DOI 10.1016/j.chembiol.2009.11.011

SUMMARY

A major challenge to studying Fe-S cluster biosynthesis in higher eukaryotes is the lack of simple tools for imaging metallocluster binding to proteins. We describe the first fluorescent approach for in vivo detection of 2Fe2S clusters that is based upon the complementation of Venus fluorescent protein fragments via human glutaredoxin 2 (GRX2) coordination of a 2Fe2S cluster. We show that *Escherichia coli* and mammalian cells expressing Venus fragments fused to GRX2 exhibit greater fluorescence than cells expressing fragments fused to a C37A mutant that cannot coordinate a metallocluster. In addition, we find that maximal fluorescence in the cytosol of mammalian cells requires the iron-sulfur cluster assembly proteins ISCU and NFS1. These findings provide evidence that glutaredoxins can dimerize within mammalian cells through coordination of a 2Fe2S cluster as observed with purified recombinant proteins.

INTRODUCTION

Proteins containing iron-sulfur (Fe-S) clusters are essential for cellular processes ranging from cytosolic regulation to mitochondrial metabolism and respiration to nuclear DNA repair (Lill, 2009). The chemistry and structure of the most common types of Fe-S centers, [2Fe2S] and [4Fe4S], have been extensively characterized (Rees and Howard, 2003). In addition, diseases have been identified that are caused by defects in proteins that contain Fe-S clusters (Finsterer, 2008) as well as those that synthesize Fe-S clusters, like Friedreich's ataxia (Campuzano et al., 1996), sideroblastic anemia (Camaschella et al., 2007), and myopathy (Mochel et al., 2008). Despite the widespread importance of metalloclusters for normal cellular function and nuclear genome stability (Veatch et al., 2009), we do not sufficiently understand the mechanisms by which Fe-S clusters are synthesized and relayed in mammalian cells to treat diseases caused by defects in their biosynthesis (Whitnall et al., 2008).

A major challenge in studying Fe-S cluster metabolism in metazoans and developing therapies for diseases caused by defects in metallocluster biosynthesis is the lack of simple imaging tools for directly monitoring the metal binding state of proteins within the individual subcellular compartments of living cells. Existing methods for studying Fe-S clusters coordinated by proteins are limited in their ability to screen for molecules that affect metallocluster homeostasis within living cells. Mössbauer and electron paramagnetic resonance spectroscopy can both detect Fe-S clusters in living cells (Djaman et al., 2004; Yang et al., 2009), but these approaches require protein overexpression and cryogenic conditions. Radiotracer studies overcome these limitations (Muhlenhoff et al., 2002). However, cell lysis and protein manipulation are required prior to analysis, restricting the throughput of this method (Pierik et al., 2009). With many metal ions, these limitations have been overcome through the development of synthetic fluorescent sensors, which can image changes in the levels of metals bound to engineered proteins (Dittmer et al., 2009) as well as their intracellular concentrations (Domaille et al., 2008). In contrast, fluorescent sensors have not been created for imaging Fe-S metalloclusters bound by proteins within the different subcellular compartments of living cells.

Recently, we showed that fluorescence spectroscopy can report on Fe-S cluster binding to purified recombinant human GRX2 (Hoff et al., 2009), a glutathione-dependent oxidoreductase that dimerizes and is inactivated in vitro through 2Fe2S coordination of an active site cysteine (Lillig et al., 2005). GRX2 retained the ability to coordinate a 2Fe2S cluster upon overexpression in *Escherichia coli* when it was fused at its N terminus to different green fluorescent protein (GFP) homologs, and 2Fe2S cluster coordination coincided with fluorescence quenching (Hoff et al., 2009). Although this study provided evidence that GFP-GRX2 will be useful as a fluorescence reporter for in vitro studies of iron-sulfur cluster assembly on GRX2 involving complex mixtures that are not compatible with existing approaches (Bonomi et al., 2008), the fluorescence changes observed upon GRX2 dimerization are not sufficient to allow for in vivo measurements of 2Fe2S-induced dimerization in the different cell types and subcellular compartments where GRX2 has been observed (Lonn et al., 2008).

To develop an assay for direct visualization of Fe-S clusters bound by GRX2 in vivo, we coupled the complementation of

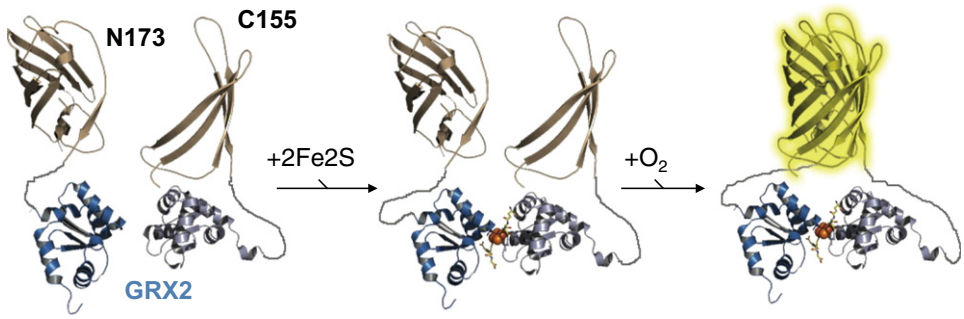

Figure 1. Strategy for Imaging GRX2 and 2Fe2S Binding

Venus fragment complementation is enhanced when GRX2 dimerizes through coordination of a 2Fe2S cluster. The dimeric structure of GRX2 is shown (Protein Data Bank ID 2HT9) (Johansson et al., 2007).

a split fluorescent protein to the synthesis of 2Fe2S clusters on GRX2 (Figure 1). In this *Fe-S* cluster *F*luorescence *A*ssay (FeSFA), nonfluorescent fragments of the yellow fluorescent protein variant Venus (Hu and Kerppola, 2003) are fused to human GRX2. The fluorescence magnitude of FeSFA is predicted to depend on the fraction of GRX2 that coordinates Fe-S clusters, because apoGRX2 is monomeric and incapable of efficiently bringing Venus fragments into close proximity for chromophore maturation.

RESULTS

Design of a Fluorescence Assay for GRX2-Bound Fe-S Clusters

A bimolecular fluorescence approach (Kerppola, 2006) was used to visualize the 2Fe2S-mediated dimerization of GRX2, because previous studies have shown that this method is sensitive to weak and transient protein-protein interactions (Magliery et al., 2005). We chose to use fragments of the yellow fluorescent protein Venus, because this protein's chromophore forms more efficiently than in other fluorescent protein variants (Nagai et al., 2002). In addition, we used polypeptide fragments of Venus, residues 1-173 (designated N173) and 155-243 (designated C155), which have previously been shown to exhibit enhanced complementation when fused to proteins that interact (Hu and Kerppola, 2003).

GRX2 Promotes Venus-Fragment Complementation in *Escherichia coli*

To demonstrate that FeSFA reports on the biosynthesis of 2Fe2S clusters, we characterized the fluorescence of Venus fragments fused at their C terminus to GRX2 lacking its mitochondrial targeting sequence (Lonn et al., 2008) and a C37A mutant of GRX2 that lacks the active-site cysteine that directly coordinates iron and promotes dimerization (Johansson et al., 2007). In addition, we examined the fluorescence of Venus fragments fused to the self-associating leucine zipper region of the yeast Gcn4 transcriptional activator as a control for Venus fragments that stably associate (Pelletier et al., 1998). Constructs were designed such that protein fusions to the C-terminal fragment of Venus (residues 155-243; termed C155) contain $(His)_6$ affinity tags whereas protein fusions to the N-terminal Venus fragment (residues 1-173; termed N173) lack affinity tags (see Figure S1 available online). We found that *Escherichia coli* coexpressing N173-GRX2 and C155-GRX2 exhibit 3.5-fold higher whole-cell fluorescence than fusion proteins harboring the C37A mutation, albeit one-third lower than the fluorescence obtained from cells expressing Venus fragments fused to Gcn4 (Figure 2A). In addition, affinity-purified C155-GRX2 coelutes from a Ni-NTA column with higher levels of N173-GRX2 than the protein fusion encoding a C37A mutation (Figure 2B). Densitometry revealed that the ratio of the N173 to $(His)_6$-C155 band intensities are 0.75 for Gcn4, 0.53 for the GRX2, and 0.31 for the C37A. Consistent with in vivo fluorescence, a lower ratio of N173 to C155 is observed with purified C155-GRX2 compared with the Gcn4-tagged Venus fragments.

To determine whether the differences in fluorescence of GRX2 and C37A protein fusions correlate with the level of Fe-S clusters coordinated by these proteins, we compared the visible circular dichroism (CD) spectra of the affinity-purified protein complexes. We found that NTA-purified protein from *E. coli* coexpressing C155-C37A and N173-C37A has a visible CD spectrum with one ellipticity minimum at 520 nm (Figure 3A). This minimum is interpreted as arising from the low levels of Venus chromophore in N173/C155 heterodimers, because the CD spectra of fluorescent, dimeric N173/C155-Gcn4 (Figure 3B) exhibits similar negative ellipticity at 520 nm, but with a much greater magnitude. C155-GRX2 complexes also display an ellipticity minimum at 520 nm that is more pronounced than that in the spectrum of C155-C37A (Figure 3C), consistent with a greater fraction of C155-GRX2 being in a complex with N173-GRX2 after purification. Furthermore, C155-GRX2 displays additional ellipticity maxima (450 nm) and minima (370 nm) that occur at similar wavelengths and relative intensities as those attributed to the 2Fe2S cluster in dimeric GRX2 (Lillig et al., 2005), implicating a direct role for 2Fe2S cluster coordination in stabilizing C155-GRX2 and N173-GRX2 complexes and promoting the maturation of the Venus chromophore.

Proximal 2Fe2S Clusters Decrease Venus Fluorescence

To investigate if 2Fe2S cluster coordination by C155-GRX2/N173-GRX2 influences the spectral properties of Venus after maturation, we purified a fusion protein composed of full-length Venus fused to GRX2 and compared the fluorescence of monomeric and dimeric Venus-GRX2. Venus-GRX2 was produced as a mixture of monomers and dimers upon overexpression in

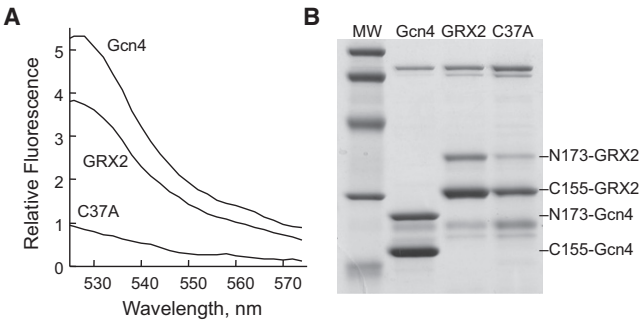

Figure 2. Analysis of Venus Fragment Association upon Overexpression in Bacteria

(A) Fluorescence spectra of *E. coli* expressing N173 and $(His)_6$ C155 Venus fragments fused to Gcn4 leucine zippers, GRX2, and a GRX2 C37A mutant that cannot coordinate 2Fe2S clusters. The spectra shown are normalized to the optical density of the cells.

(B) SDS PAGE analysis of $(His)_6$ C155 Venus fragments (10 μg each) that were Ni NTA purified from *E. coli* coexpressing pairs of N173 and $(His)_6$ C155 fragments fused to Gcn4, GRX2, and C37A. Molecular weight markers: 21.5, 31, 45, 66.2, and 97.4 kDa.

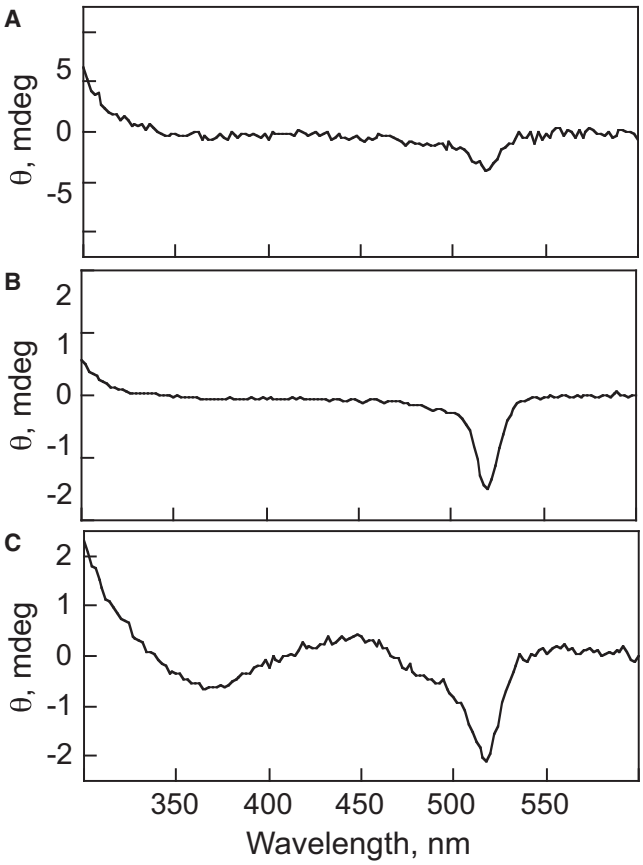

Figure 3. Circular Dichroism Spectra of Purified Venus Fusion Protein Complexes

Visible circular dichroism spectra of purified (A) C155 C37A, (B) C155 Gcn4, and (C) C155 GRX2 (1 mg each) were acquired at 25°C using protein complexes purified from *E. coli* coexpressing pairs of $(His)_6$ C155 and N173 fusion proteins. All data were corrected for the ellipticity of the buffer. The large ellipticity minimum in the complex of $(His)_6$ C155 Gcn4/N173 Gcn4 is attributed to the mature Venus fluorophore.

E. coli (Figure S2A). CD analysis of these different proteins revealed that the monomer lacks an Fe-S cluster (Figure S2B), whereas the dimer contains bound 2Fe2S cluster (Figure S2C) like native GRX2 (Lillig et al., 2005). In addition, the 2Fe2S-cluster bound dimer of Venus-GRX2 exhibits a 30% reduction in fluorescence compared to the monomer (Figure S2D), which is smaller in magnitude than that previously observed with other fluorescent proteins fusions (Hoff et al., 2009). To examine whether this decrease in fluorescence arises from the proximity of the neighboring Venus chromophores, we also purified a fusion protein having Venus fused to Gcn4 via a linker containing an enterokinase cleavage site. Enterokinase treatment for 48 hr converted Venus-Gcn4 from a dimer to a near equal mixture of monomer and dimer (Figures S3A and S3B). In addition, the enterokinase-treated protein exhibited ~10% lower fluorescence than mock-treated protein (Figure S3C). The magnitude of this quenching is smaller than that of Venus-GRX2 upon dimerization, indicating that fluorophore proximity and transition metal quenching both contribute to the lower fluorescence of C155-GRX2/N173-GRX2 compared with Venus fragments fused to Gcn4.

GRX2-Induced Venus Fluorescence Is Irreversible

To establish whether GRX2-mediated Venus fragment complementation is irreversible, we examined the effect of 2Fe2S removal on the fluorescence of a purified complex of C155-GRX2/N173-GRX2. Metallocluster dissociation was induced by addition of ascorbate, a reductant known to destabilize the metallocluster (Lillig et al., 2005), while not affecting the fluorescent p-hydroxybenzylidene-imidazolidone moiety within intrinsically fluorescent proteins (Hoff et al., 2009). CD analysis revealed that addition of ascorbate induces a time-dependent loss of the 2Fe2S cluster coordinated by C155-GRX2/N173-GRX2 (Figure 4A) and a ~10% increase in fluorescence (Figure 4B). The $t_{1/2}$ for both spectral transitions occurred 0.86 hr after ascorbate treatment (data not shown). These in vitro findings provide evidence that our Fe-S fluorescence assay is irreversible as previously observed in fluorescent protein fragment complementation assays (Magliery et al., 2005), and they show that FeSFA is suitable for detecting 2Fe2S clusters that are transiently coordinated by GRX2. In addition, these results provide additional evidence that 2Fe2S binding by GRX2 weakly quenches the fluorescence of Venus.

GRX2 Enhances Venus-Fragment Complementation in Mitochondria

We next investigated whether FeSFA can monitor Fe-S cluster biosynthesis reactions in mammalian cells. Because the dominant mitochondrial GRX2 isoform (GRX2a) is ubiquitously expressed (Lonn et al., 2008), we first characterized the fluorescence of HEK293 cells transiently cotransfected with constructs expressing N173 and C155 fusion proteins with mitochondrial localization tags (Figure S4). In all three cases, confocal images reveal that Venus fluorescence colocalizes with the mitochondria-specific dye MitoTracker Red (Figure 5A), and visual

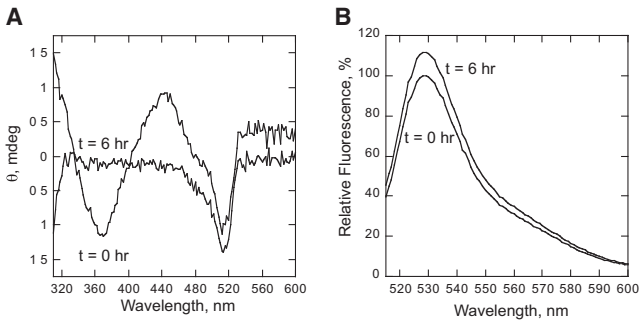

Figure 4. Reversibility of GRX2 Mediated Venus Fragment Complementation

(A) Incubation of purified, recombinant N173 GRX2/C155 GRX2 with 5 mM ascorbate leads to loss of the ellipticity minima (370 nm) and maxima (450 nm) that are observed in the spectrum of 2Fe2S bound dimers of GRX2 (Lillig et al., 2005).

(B) Incubation of purified N173 GRX2/C155 GRX2 with 5 mM ascorbate leads to an increase in Venus fluorescence. All samples were baseline corrected for buffer ellipticity and fluorescence.

inspection indicates that cells expressing Venus fragments fused to Gcn4 and GRX2 display enhanced fluorescence relative to C37A fusions. Flow cytometry analysis reveals that cells coexpressing N173-GRX2 and C155-GRX2 also exhibit 12-fold higher average Venus fluorescence than cells expressing the protein fusions harboring the C37A mutation in GRX2 (Figure 5B), greater than the difference observed in *E. coli*. The higher fluorescence with GRX2 fusion proteins is interpreted as arising from 2Fe2S-induced dimerization of Venus fragments, because the GRX2 constructs are not transcribed to a greater extent than those that contain the C37A mutation (Figure 6A), the GRX2 and C37A fusions proteins accumulate to a similar extent (Figure 6B), and cells transfected with each fusion pair display similar viability to mock-transfected cells (data not shown). As observed in the bacterial studies, cells expressing N173-Gcn4 and C155-Gcn4 exhibit higher fluorescence than cells producing the GRX2-fused fragments.

GRX2 Enhances Venus-Fragment Complementation in the Cytosol

Cystosolic glutaredoxin 2 has recently been implicated as having a role in iron-sulfur cluster coordination (Lonn et al., 2008), but the ability of this protein to coordinate iron-sulfur clusters in vivo has not been established. To directly test this using FeSFA, we built constructs for coexpressing N173 and C155 fusion proteins lacking mitochondrial localization signals (Figure S4), and we examined their fluorescence in HEK293 cells. All three N173/C155 Venus fragment pairs exhibit diffuse fluorescence characteristic of cytosolic proteins (Figure 5A). In addition, flow cytometry analysis of cells expressing cytosolic Venus fragments display similar differences in average fluorescence as observed with bacterial and mitochondrial constructs (Figure 5B): Gcn4 > GRX2 > C37A. Cells coexpressing N173-GRX2 and C155-GRX2 exhibit 8.2-fold higher average Venus fluorescence than cells expressing the protein fusions harboring the C37A mutation in GRX2. As in the mitochondria, the observed fluorescence difference between cytosolic GRX2 and C37A constructs does not arise from greater accumulation of GRX2 transcripts or fusion proteins (Figures 6A and 6B).

Fe-S Cluster Assembly Is Required for Maximal Venus Fluorescence

To investigate whether the fluorescence signal of our cytosolic-localized FeSFA arises from 2Fe2S-mediated dimerization of GRX2, we used RNA interference to deplete two Fe-S cluster assembly proteins and compared the effects of depletion on the fluorescence of Venus fragments fused to GRX2 and C37A. The cysteine desulfurase NFS1 and iron-sulfur cluster template ISCU were targeted using short interfering RNAs (siRNAs) because their depletion has been shown to cause cytosolic defects in Fe-S cluster biogenesis (Fosset et al., 2006; Song and Lee, 2008; Tong and Rouault, 2006). Transfection of HEK293 cells with siRNAs corresponding to those previously reported lead to a > 50% reduction in NFS1 and ISCU levels compared to cells treated with a mock siRNA (Figure 7A). In addition, NFS1 and ISCU depleted cells show a significant reduction (>50%) in the fluorescence obtained from Venus fragments fused to GRX2 compared with mock-treated cells (Figure 7B) and a decrease in the activity of xanthine oxidase, an enzyme that requires an Fe-S cluster to function (Figure S5). In contrast, the levels of transcripts encoding Venus fragment fusion proteins were not similarly affected (Figure 7C), demonstrating that the changes in fluorescence are not due to differences in gene expression. These results indicate that dimerization of GRX2 in the cytosol requires iron-sulfur assembly proteins, and that the Venus fragment assembly trap has utility for detecting cellular defects in Fe-S cluster biosynthesis.

DISCUSSION

Monothiol and dithiol glutaredoxins have both been implicated as essential for maintaining Fe-S cluster homeostasis in eukaryotes. In yeast, depletion of the monothiol glutaredoxin Grx5p leads to a decrease in Fe-S cluster protein activities and the accumulation of Fe-S clusters coordinated by the mitochondrial template protein Isu1p (Muhlenhoff et al., 2003). This suggests that monothiol glutaredoxins may play a role in regulating Fe-S cluster biogenesis after initial assembly on template proteins. In mammals, the activities of Fe-S cluster proteins are also decreased by a mutation in the monothiol GLRX5 (Camaschella et al., 2007) as well as depletion of the dithiol GRX2 (Lee et al., 2009). In vitro studies have provided evidence that these phenotypes may arise because glutaredoxins require a direct interaction with Fe-S clusters to maintain homeostasis. Monothiol and dithiol glutaredoxins have both been shown to form 2Fe2S-bridged dimers upon overexpression in bacteria (Lillig et al., 2008), and these findings have implicated possible roles for metalloclusters in regulating the oxidoreductase activities of glutaredoxins (Lillig et al., 2005) and for glutaredoxins in delivering Fe-S clusters to apo-acceptor scaffold proteins (Bandyopadhyay et al., 2008). To date, however, no direct evidence for glutaredoxin dimers has been reported within living eukaryotes, although GRX2 has been shown to coimmunoprecipitate with ^{55}Fe from tissue culture cells (Lillig et al., 2005).

Herein we provide the first direct evidence that a dithiol glutaredoxin self-associates through a metallocluster within human

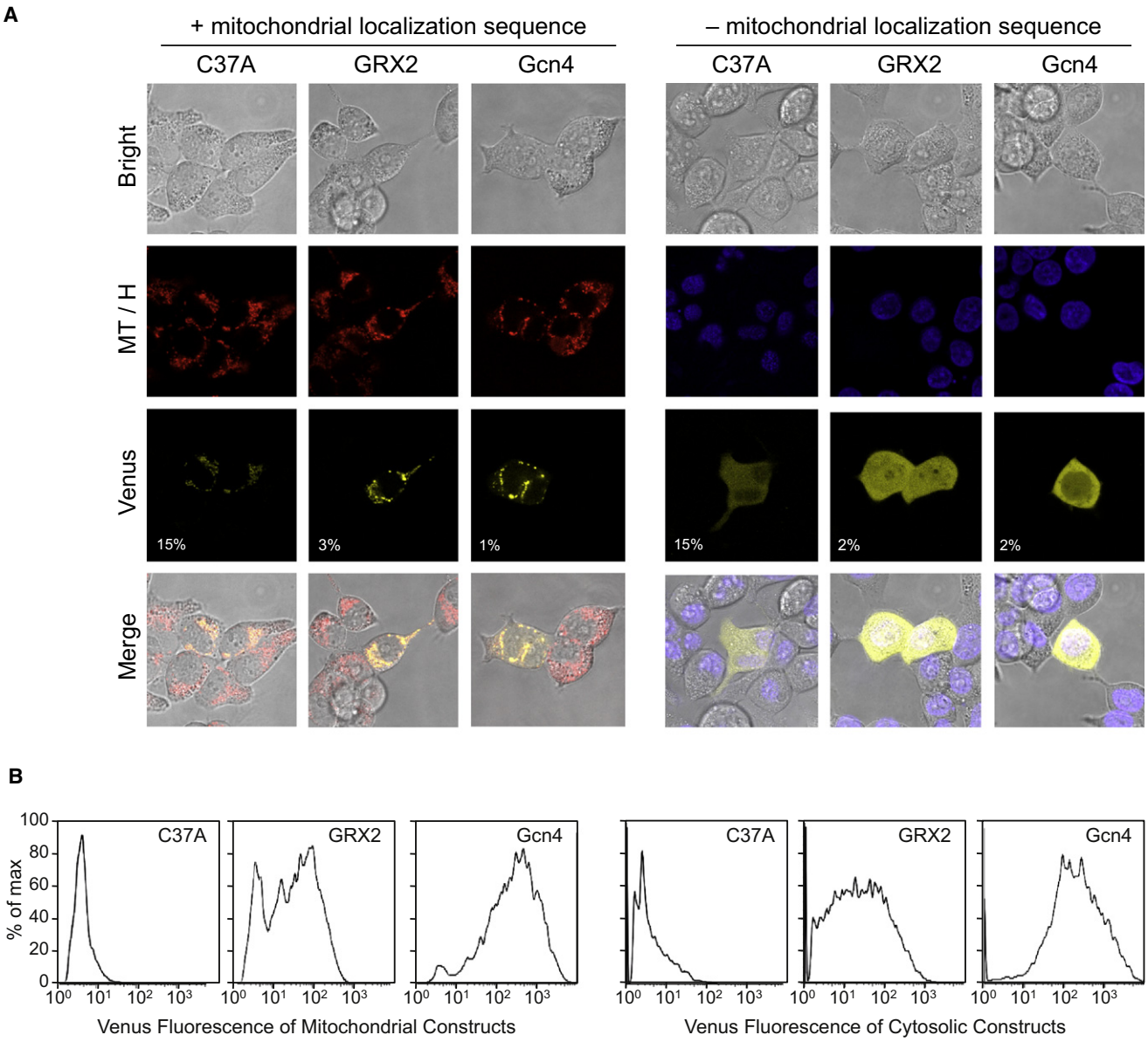

Figure 5. Venus Fluorescence in HEK293 Cells

(A) Confocal images of HEK293 cells coexpressing Venus fragments fused to Gcn4, GRX2, and C37A were obtained using a 63x, 1.4NA objective lens. Mitochon drial constructs (left) colocalize with MitoTracker Red (MT) while cytosolic constructs (right) display diffuse staining. Bright field images are shown to demonstrate cell health and visualize the location of all cells, and Hoechst (H) nuclear stain is shown for reference with cytosolic constructs. To obtain images that show the Venus localization of our different constructs, the percentage transmission of the excitation laser light was adjusted to the values shown on the Venus images. (B) The fluorescence of cells transiently transfected with vectors that express mitochondrial (left) and cytosolic (right) Venus fragment pairs fused to Gcn4, GRX2, and GRX2 C37A was determined using flow cytometry. Cells were cotransfected with Venus fragment constructs and a plasmid that constitutively expresses the cyan fluorescent protein (Cy PET). Venus fluorescence is only shown for those cells that exhibit detectable Cy PET fluorescence The mitochondrial constructs yielded mean arbitrary fluorescence values of 6.0 ± 0.2 (GRX2 C37A), 71 ± 1.9 (GRX2), and 554.6 ± 9.2 (Gcn4). The cytosolic constructs yielded mean fluores cence values of 8.2 ± 1.6 (GRX2 C37A), 67.5 ± 7.5 (GRX2), and 522.0 ± 19.5 (Gcn4). Fluorescence values were determined from three independent experiments and are reported ± 1 standard deviation.

cells. Cells coexpressing Venus fragments fused to GRX2 in either the mitochondria or the cytosol were found to exhibit higher fluorescence than those expressing proteins fusions with the iron ligand (Cys37) mutated to alanine (Johansson et al., 2007). In the cytosol, the increased fluorescence of GRX2 fusions compared with constructs having the C37A mutation is attributed to 2Fe2S binding, because the ratio of GRX2 to C37A fluorescence is less pronounced upon depletion of proteins that are required for the synthesis of other cytosolic iron-sulfur clusters (Fosset et al., 2006; Tong and Rouault, 2006). In the mitochondria, the higher fluorescence with GRX2 protein fusions compared with the C37A mutants is also

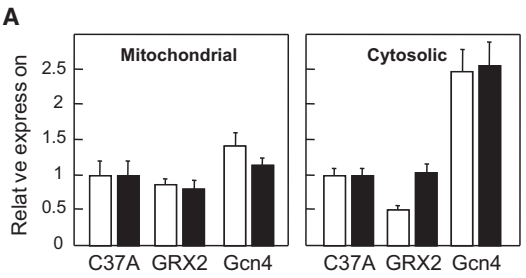

Figure 6. Protein and Transcript Levels in Transiently Transfected Cells

(A) Quantitative PCR analysis of Venus *N173* (white) and *C155* (black) transcripts in HEK293 cells. Transcript levels are reported relative to *C37A* levels in each cellular compartment. Error bars represent one standard deviation.

(B) Western immunoblots showing the relative levels of GRX2 and C37A protein fusions in HEK293 cells cotransfected with vectors that ex press N173 and C155 fragments fused to GRX2 and C37A.

attributed to 2Fe2S cluster binding, because GRX2 coimmunoprecipitates with ^{55}Fe in cells that are only predicted to express the mitochondrial isoform of this protein (Lillig et al., 2005). Taken together, these finding suggest that the ratio of GRX2 to C37A fluorescence can be used in cells depleted for known Fe-S cluster assembly proteins (Lill, 2009) to identify the proteins required for the biosynthesis of 2Fe2S clusters on GRX2. In addition, this approach will be useful for determining if the level of Fe-S clusters bound by GRX2 is altered in cell models for mitochondrial diseases, such as Friedreich's ataxia (Calmels et al., 2009).

A comparison of our results with expression analysis of the three human GRX2 isoforms (GRX2a, GRX2b, and GRX2c) suggests that Fe-S clusters regulate the activity of two of these isoforms under physiological conditions. The glutaredoxin that we used to drive Venus-fragment complementation is identical in sequence to the mitochondrial isoform (GRX2a) after removal of its mitochondrial targeting sequence (Lundberg et al., 2001). The ubiquitous expression pattern of *GRX2a* suggests that Fe-S clusters may play a housekeeping role in regulating the function of this isoform in all cell types (Lonn et al., 2008). The glutaredoxin that we fused to Venus fragments is also identical to GRX2c, an isoform that localized to the cytosol and nucleus (Lonn et al., 2008). Unlike *GRX2a*, however, *GRX2c* transcripts are restricted to the testis in healthy tissues and cancer cells (Hudemann et al., 2009), implicating a more limited role for Fe-S cluster regulation of this cytosolic isoform. Future studies will be required to test whether GRX2a and GRX2c coordinate Fe-S clusters in all of the tissues where they are expressed and to establish the cellular role(s) for metallocluster binding.

Our measurements of Venus-fragment complementation within *E. coli* also provides evidence that fluorescence imaging can report on 2Fe2S binding to glutaredoxins within prokaryotes. Bacteria expressing GRX2 and Venus fragment fusions exhibit greater fluorescence than those with a C37A mutation that prevents 2Fe2S binding (Johansson et al., 2007), albeit less than the Gcn4 fused fragments that associate without the assistance of an Fe-S cluster (O'Shea et al., 1991). In addition, His-tagged C155-GRX2 copurifies with more N173-GRX2 than protein fusions containing the C37A mutation, and only the GRX2 complex contains a 2Fe2S cluster. These findings indicate that FeSFA can be used in *E. coli* to screen libraries of GRX2 mutants created by error-prone polymerase chain reaction (PCR) for variants that retain the ability to dimerize through a 2Fe2S cluster (Bloom et al., 2005). In addition, our findings suggest that Venus-fragment complementation will be useful for testing whether monothiol glutaredoxins coordinate 2Fe2S clusters in vivo as predicted from in vitro reconstitution studies (Iwema et al., 2009). Furthermore, the Venus fragment assembly trap is predicted to be useful for discovering proteins that form transient Fe-S cluster bridged heterodimers with glutaredoxins (Li et al., 2009). In vitro studies have implicated a role for Fe-S scaffold proteins in transferring metallocluster to other proteins (Bonomi et al., 2008), but intermediates that form during cluster transfer have not yet been observed.

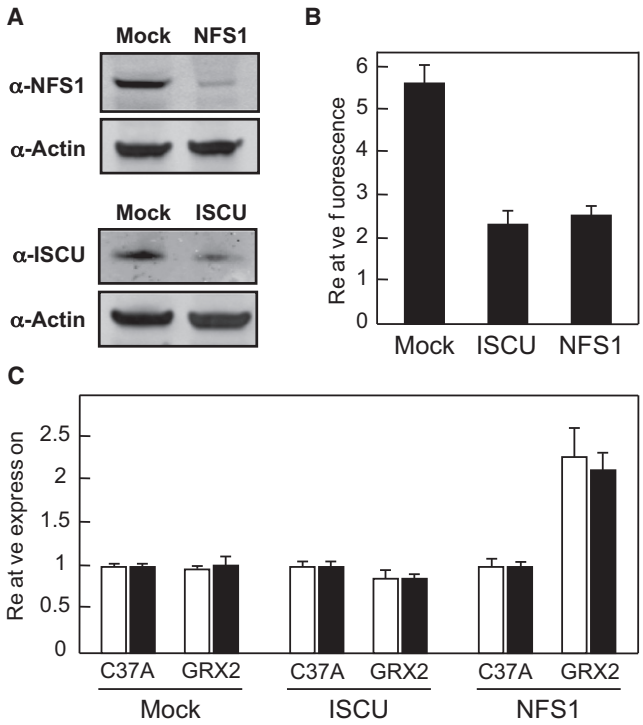

Figure 7. ISCU and NFS1 Are Needed for Maximal Venus Fragment Complementation in the Cytosol

(A) Western immunoblotting to ISCU and NFS1 in cells transfected with a siRNA duplex targeted to *ISCU*, *NFS1,* and a mock siRNA that does not target any human genes. Immunodetection of actin is shown as a load control.

(B) Relative fluorescence of cytosolic GRX2 and C37A Venus fragment pairs in mock, NFS1 depleted, and ISCU depleted HEK293 cells was determined using flow cytometry. Fluorescence is reported relative to that observed for the C37A constructs.

(C) Quantitative PCR analysis of Venus *N173* (white) and *C155* (black) tran scripts in HEK293 cells that have been transfected with a siRNA duplex targeted to *ISCU*, *NFS1,* and a mock siRNA. Transcript levels are reported relative to C37A levels. Error bars represent one standard deviation.

Studies examining the stability of the fluorescent N173-GRX2/C155-GRX2 complex demonstrate that the signal arising from GRX2 dimerization is irreversible, as observed in previous bimolecular fluorescence complementation studies (Stefan et al., 2007). This attribute will preclude the use of FeSFA to continuously monitor dynamic changes in GRX2 dimerization, although regulated protein expression can be used to control when the fluorescence signal begins to accumulate. Such a strategy has been effective for analyzing inhibitors of protein-protein interactions in other bimolecular fluorescence complementation studies (Morell et al., 2008). The detection of dynamic changes in GRX2 dimerization (and 2Fe2S binding) may be achievable using luciferase-fragment complementation (Stefan et al., 2007) and fluorescence resonance energy transfer (Greeson et al., 2006). However, these methods could experience greater issues with signal to noise compared with FeSFA, especially under cellular conditions where only a fraction of GRX2 coordinates a transient 2Fe2S cluster. Ongoing studies are examining the tradeoff between reporter sensitivity and time-resolved information obtained from different dimerization reporters.

SIGNIFICANCE

In nature, specialized proteins have evolved to synthesize and relay iron-sulfur clusters to proteins that require these metalloclusters to function (Lill, 2009). Biochemical and genetic studies in bacteria (Raulfs et al., 2008) and fungi (Lill and Muhlenhoff, 2008) have provided insight into the mechanism of these reactions in living cells. However, our understanding of these processes in mammals is far more limited because of inherent limitations in the biochemical (Pierik et al., 2009) and biophysical techniques (Djaman et al., 2004; Yang et al., 2009) available to study protein-bound iron-sulfur clusters in cell models. Here we show that the relative levels of 2Fe2S clusters coordinated by human GRX2 can be imaged in mammalian tissue culture cells using bimolecular fluorescence complementation (Kerppola, 2006). Because of the relative ease of this approach and the array of accessible instrumentation with which it can be employed (e.g., fluorimeters, flow cytometers, and fluorescent microscopes), we propose that it will aid in discovering additional glutaredoxins that coordinate Fe-S cluster in living cells (Lillig et al., 2008) and determining the extent to which GRX2 binding to Fe-S clusters is altered in cell models of human diseases (Calmels et al., 2009). With appropriate high-throughput screening, this approach should aid in identifying proteins whose depletion (and overexpression) affect iron-sulfur cluster homeostasis in the different subcellular compartments where glutaredoxins are found (Lonn et al., 2008).

EXPERIMENTAL PROCEDURES

Plasmid Construction

A gene fusion encoding full length Venus (residues 1 243) (Nagai et al., 2002) fused to the N terminus of the processed mitochondrial isoform of GRX2 (residues 42 164) (Gladyshev et al., 2001) through a 15 amino acid $(GGGGS)_3$ linker was generated by PCR assembly (Horton et al., 1989) and cloned into pET28a (EMD Biosciences) using bamHI and notI sites to produce a vector that expresses a fusion protein with a N terminal $(His)_6$ tag. In addition, a gene fusion encoding the dimerizing region of the Gcn4 leucine zipper (residues 245 281) (O'Shea et al., 1991) connected to the C terminus of Venus (Nagai et al., 2002) through a DDDDK $(GGGGS)_3$ linker was cloned into pET28a using bamHI and notI sites. This vector expresses a Venus protein fusion with a N terminal $(His)_6$ tag and a linker containing an enterokinase cleavage site.

Bacterial vectors for expressing N173 protein fusions were generated by cloning genes encoding Venus residues 1 173 fused to Gcn4, GRX2, and C37A through a 15 amino acid $(GGGGS)_3$ linker into pET21d (EMD Biosciences) using bamHI and notI sites. Plasmids for expressing C155 protein fusions in *E. coli* were constructed by cloning genes encoding Venus residues 155 243 fused to Gcn4, GRX2, and C37A through a $(GGGGS)_3$ linker into pET28a using bamHI and notI sites. All pET28 derived vectors produce proteins having a $(His)_6$ tag at their N terminus, whereas pET21 derived vectors express proteins without an affinity tag.

Mammalian expression vectors were constructed through PCR assembly as for bacterial constructs, but with the inclusion of a single copy of either the FLAG (Venus N173 constructs) or Myc epitope (Venus C155 constructs) at the C terminus of the fusion protein. All constructs were cloned into pcDNA5/frt (Invitrogen) using bamHI and notI restriction sites. Mitochondrial localization sequences were added in frame at the N termini of cytosolic constructs by ligating a synthetic oligonucleotide encoding the cytochrome c oxidase subunit 8 mitochondrial localization sequence (Huttemann et al., 2003) into unique ecoRI and bamHI sites. All constructs were verified by DNA sequencing.

Bacterial Expression and Protein Purification

E. coli BL 21 (DE3) RIL cells harboring vectors for coexpressing N173 and C155 Venus fusion proteins were grown in LB containing 50 μg/ml ampicillin and 10 μg/ml kanamycin at 30°C, induced with 1 mM IPTG at $A_{600} \approx 1$, and grown for exactly 60 min at 30°C. Harvested cells were resuspended in PSIG (50 mM phosphate [pH 7.0], 300 mM NaCl, 10 mM imidazole, 2 mM GSH) containing 1 mM $MgCl_2$, 300 μg/ml lysozyme, and 2 U/ml DNase I. Resuspended cells were frozen at −80°C, thawed, and centrifuged at 15k × g for 1 hr. Cleared lysate was applied to a 2 ml nickel talon affinity (NTA) column (QIAGEN) equilibrated with PSIG, washed with 50 column volumes of PSIG, and protein was eluted using exactly 3 ml PSIG containing 250 mM imidazole. Samples eluted from the column were immediately used for spectral measurements at 23°C. To obtain a buffer control for baseline corrections of spectra, a column equilibrated with PSIG was washed with exactly 3 ml PSIG containing 250 mM imidazole. To facilitate rapid analysis of protein ellipticity and fluorescence before significant proteolytic degradation could occur, the concentrations of the purified proteins were assessed using the Bradford method with bovine serum albumin (BSA) as a standard. This approach was chosen over spectrophotometric quantitation because the buffer used to elute proteins from NTA resin contains 250 mM imidazole. Imidazole absorbs at the same wavelength as tyrosine and tryptophan, preventing any absorption measurements without a time consuming and potentially damaging dialysis step. Protein purity was analyzed by electrophoresis on a NuPAGE 10% Bis Tris SDS PAGE gel (Invitrogen) with MOPS SDS running buffer.

Spectroscopy

A Varian Cary 50 UV/Vis spectrophotometer was used for absorbance measurements. Circular dichroism spectra were recorded at 25°C using a JASCO 815 spectropolarimeter with a 1 cm path length cuvette using a 4 nm bandwidth. All CD spectra shown are corrected for the ellipticity of the buffer. Whole cell fluorescence spectra of bacteria expressing each N173 and C155 fragment pair were measured 1 hr after induction using a Tecan Safire plate reader ($\lambda_{excitation}$ = 505 nm). Fluorescence spectra of purified proteins were recorded at 25°C using an SLM AMINCO Series 2 spectropolarimeter using a path length of 1 cm, a 4 nm bandwidth, and a $\lambda_{excitation}$ = 510 nm.

Effect of Enterokinase on Venus-Gcn4

A sample of Venus Gcn4 (20 μM) in PSG buffer was divided into two samples, 4 U enterokinase (Novagen) was added to one sample, and an equivalent volume of buffer was added to the other sample. After incubation at room temperature for 48 hr, the fraction of protein cleaved in each sample was analyzed by SDS PAGE and gel filtration chromatography on a Superdex 75

column. In addition, the fluorescence of these samples was compared using a $\lambda_{excitation}$ = 510 nm.

Venus Fragment Complex Stability Measurements

Because aggregation prone monomeric C155 GRX2 copurifies with the 2Fe2S complex of N173 GRX2/C155 GRX2 during NTA chromatography, NTA purified C155 GRX2 was chromatographed on a Superdex 75 gel filtration column that had been equilibrated in PSIG buffer. Fractions migrating at the apparent molecular weight of the protein complex, which were fluorescent and found by SDS PAGE to contain equimolar amounts of N173 GRX2 and C155 GRX2, were pooled and immediately transferred to glutathione free PSI buffer using a 5 ml HiTrap desalting column (GE Healthcare). Ascorbate was added to the eluted protein to a final concentration of 5 mM, and protein ellipticity and fluorescence was monitored. As previously observed, the 2Fe2S cluster bound to GRX2 was destabilized by ascorbate, although the kinetics of Fe S cluster loss from the N173 GRX2/C155 GRX2 complex was faster than that reported for purified, dimeric GRX2 (Lillig et al., 2005). In addition, the fluorescence of the N173 GRX2/C155 GRX2 complex was found to increase ~10% with a rate that mirrored the loss of the 2Fe2S dependent ellipticity. Because the buffer conditions required for metallocluster destabilization involved conditions that could lead to intermolecular disulfides between active site cysteines in fluorescent complexes of N173 GRX2 and C155 GRX2, we examined the effect of adding excess dithiothreitol (10 mM) to the protein complex immediately after 2Fe2S dissociation. A 15 hr incubation with dithiothreitol did not lead to any reduction in the Venus fluorescence (data not shown).

Confocal Microscopy

HEK293 cells were cultured in Dulbecco's modified Eagle's medium (DMEM) supplemented with 10% bovine calf serum at 37°C in a 90% humidified atmosphere containing 5% CO_2. Cells were seeded in 6 well plates and allowed to reach 80% confluency before transfection with pairs of plasmids that constitutively express the different Venus fragment pairs (*i.e.*, C155 and N173 fused to Gcn4, GRX2, and C37A, respectively). Transfections were performed using 2 μg each plasmid and 6 μl Fugene6 transfection reagent (Roche). After an 8 hr exposure to transfection reagents, cells were replated to glass bottom dishes (MatTek Corp) for imaging at 24 hr after transfection. Cells were stained with either 50 nM MitoTracker Red CMXRos (Invitrogen) or 5 μg/ml Hoechst 33342 (Invitrogen) in phosphate buffered saline (PBS) at 23°C for 20 min. After washing with PBS, live cells were imaged using an LSM 510 confocal fluorescence microscope (Carl Zeiss, Inc). Venus and Mitotracker Red were excited with Argon (514 nm) and HeNe (543 nm) lasers, respectively, and using dichroics and filters (bandpass and longpass) the Venus and MitoTracker fluorescence was isolated in separate channels spanning 545 590 nm and greater than 560 nm, respectively. To obtain clear images of Venus fluorescence, the percentage transmission of excitation laser light was varied from 1% to 15%. Hoechst was excited using a Ti:Sapphire 2 photon laser (Coherent, Inc.) tuned to 750 nm, and emission of this nuclear dye was captured by a channel spanning 435 485 nm. The pinhole for the MitoTracker channel was set to 4 Airy units, the pinhole for the Venus channel was set to 2 or 4 Airy units to image the mitochondrial or cytosolic localized constructs, and the pinhole was completely open when using two photon excitation with the Hoechst dye.

Flow Cytometry

HEK293 cells analyzed by flow cytometry were cotransfected with pairs of plasmids (225 ng each) that constitutively express the different Venus fragment pairs (i.e., C155 and N173 fused to Gcn4, GRX2, and C37A, respectively) and a plasmid (pCEP4CyPet MAMM, Addgene plasmid #14033) that constitutively expresses the cyan fluorescent protein Cy PET (50 ng). The cells were harvested by trypsinization, pooled, and analyzed on a Beckman Coulter Quanta flow cytometer 24 hr after transfection. Cy PET fluorescence was obtained by using a mercury arc lamp with a 425/40 nm filter for excitation and a 480/40 nm filter for detection, whereas Venus fluorescence was obtained using a 488 nm laser for excitation and a 525/40 nm filter for detection. Viable cells were gated based on their side scatter, and the percentage of Cy PET fluorescent cells was calculated using only those viable cells that exhibited fluorescence greater than the gated untransfected population of HEK293 cells. Venus fluorescence is only shown for the subpopulation of each transfection that were found to exhibit CyPET fluorescence. All data analysis was performed using FlowJo 7.4.2 software.

Cell Viability Measurements

To investigate whether Venus fragments fused to GRX2 and C37A are toxic to the HEK293 cells used for analysis, we compared the viability of cells transfected with our reporters to mock transfected cells by flow cytometry using 7 Amino Actinomycin D (7 AAD; Invitrogen). Cells were harvested by trypsinization 24 hr after transfection, and 1 μg 7 AAD was added to each sample. Cells were then analyzed for 7 AAD incorporation, a measure of cell death, by flow cytometry with 488 nm laser excitation and 610 nm long pass emission filter. Under our assay conditions, all transfected cell populations exhibited similar viability of ~80% (data not shown).

RNA Interference-Mediated Gene Silencing

HEK293 cells maintained in DMEM supplemented with 10% bovine calf serum at 37°C in a 90% humidified atmosphere containing 5% CO_2 in 24 well plates and allowed to reach 50% confluency before transfection with 20 nM duplex RNA molecules directed toward *NFS1* (CAAGUAGCAUCUCUGAUUG) (Song and Lee, 2008), *ISCU* (UCAAGGCCGCCCUGGCUGA) (Tong and Rouault, 2006), or mock Accel Non targeting siRNA #3 (Dharmacon, Catalog # D 001910 03 05) using lipofectamine RNAiMAX (Invitrogen) as recommended by the manufacturer. After 3 days growth, cells were split 1 to 4 and reverse transfected with 20 nM RNA duplexes. After 1 day of growth, cells were transfected with Grx2 and GRX2 C37A sensor pairs (225 ng each) and pCY Pet MAMM (100 ng) using Fugene6. Cells were collected for flow cytometry and western blotting 18 hr after transfection.

Quantitative PCR

Total cellular RNA was purified from transiently transfected HEK293 cells using GenElute mammalian total RNA purification kit (Sigma) according to the manufacturer's instructions, followed by DNase treatment (Invitrogen). cDNA was synthesized using a gene specific primer for the pcDNA5/frt vector and Superscript III reverse transcriptase (Invitrogen) according to the manufacturer's instructions. Quantitative real time PCR analysis was performed using primers specific for the transcripts encoding N173 and C155 fragments (Table S1). Reactions were 25 μl and contained 1 μl template cDNA, 10 pmol each primer, and 1X iQ SYBR green supermix (Bio Rad). Reactions were carried out using an iCycler iQ system (Bio Rad) for 30 cycles (95°C for 15 s, 72°C for 30 s). The purity of the PCR products was determined by melt curve analysis. Data analysis was completed using the iCycler IQ system software v.3.1.7050 (Bio Rad). The relative expression of the N173 and C155 Venus fragments was calculated using the ΔCt (change in cycling threshold) method (Livak and Schmittgen, 2001). Expression levels were normalized to the levels of HPRT (hypoxanthine guanine phosphoribosyltransferase). Fold expression data are reported as the mean expression for each sample divided by the mean expression of the corresponding C37A construct ± 1 standard deviation.

Western Immunoblots

Whole cell extracts were prepared from harvested cells using M PER mammalian protein extraction reagent (Pierce) supplemented with 0.1 mM PMSF, and total protein concentrations were determined using Bradford Coomassie reagent (Bio Rad) with BSA as a standard. Equal amounts of protein (50 μg) were resolved on Nu PAGE 4% 12% SDS PAGE gels (Invitrogen) using MES SDS buffer and transferred to Protran nitrocellulose membranes (Whatman) using the Trans Blot SD semi dry transfer cell (Bio Rad). After blocking with 5% BSA in TBST (50 nM Tris [pH 8.0], 150 nM NaCl, 0.1% Tween 20) overnight, the membranes were incubated with the specified antibodies at 20°C. After incubation, the membranes were washed with TBST and then incubated with the corresponding secondary antibody conjugated with HRP. Signals were detected using the ECL plus western blotting substrate (GE Healthcare) according to the manufacturer's protocol. Western immunoblots were performed using mouse monoclonal antibodies to human NFS1 (1:500 dilution, Santa Cruz Biotech) and detected with a 1:10,000 dilution of goat anti mouse HRP secondary (Santa Cruz Biochem) and to the Flag (1:2,000 dilution, Sigma Aldrich) and Myc epitopes (1:10,000 dilution, Sigma Aldrich) and detected with a 1:10,000 or 1:40,000 dilution of

goat anti mouse HRP secondary (Santa Cruz Biochem), respectively. ISCU was detected with affinity purified rabbit polyclonal antibody toward *E. coli* IscU (1:100 dilution, kind gift from Larry E. Vickery, University of California, Ir vine) (Hoff et al., 2000) and detected with a 1:40,000 mouse anti rabbit HRP conjugate (Sigma Aldrich). Actin was detected with a goat polyclonal antibody toward α actin (1:1,000 dilution, Santa Cruz Biotech) detected with a 1:10,000 dilution of donkey anti goat HRP secondary (Santa Cruz Biochem).

SUPPLEMENTAL DATA

Supplemental Data include five figures and Supplemental Experimental Proce dures and can be found with this article online at: http://www.cell.com/ chemistry biology/supplemental/S1074 5521(09)00402 5.

ACKNOWLEDGMENTS

This work was supported by the American Heart Association and the Friedreich's Ataxia Research Alliance #09BGIA2220299 (to J.J.S.), Arnold and Mabel Beckman Foundation, and the Caltech Joseph Jacobs Institute for Molecular Engineering for Medicine (to C.D.S.), the Robert A. Welch Foun dation C 1614 (to J.J.S.), and the National Institutes of Health fellowship 5F32GM078901 (to K.G.H) and training grant 2T32 GM008362 (to P.Q.N.).

Received: September 9, 2009
Revised: October 28, 2009
Accepted: November 2, 2009
Published: December 23, 2009

REFERENCES

Bandyopadhyay, S., Gama, F., Molina Navarro, M.M., Gualberto, J.M., Clax ton, R., Naik, S.G., Huynh, B.H., Herrero, E., Jacquot, J.P., Johnson, M.K., and Rouhier, N. (2008). Chloroplast monothiol glutaredoxins as scaffold proteins for the assembly and delivery of [2Fe 2S] clusters. EMBO J. *27*, 1122 1133.

Bloom, J.D., Silberg, J.J., Wilke, C.O., Drummond, D.A., Adami, C., and Arnold, F.H. (2005). Thermodynamic prediction of protein neutrality. Proc. Natl. Acad. Sci. USA *102*, 606 611.

Bonomi, F., Iametti, S., Morleo, A., Ta, D., and Vickery, L.E. (2008). Studies on the mechanism of catalysis of iron sulfur cluster transfer from IscU[2Fe2S] by HscA/HscB chaperones. Biochemistry *47*, 12795 12801.

Calmels, N., Schmucker, S., Wattenhofer Donze, M., Martelli, A., Vaucamps, N., Reutenauer, L., Messaddeq, N., Bouton, C., Koenig, M., and Puccio, H. (2009). The first cellular models based on frataxin missense mutations that reproduce spontaneously the defects associated with Friedreich ataxia. PLoS ONE *4*, e6379.

Camaschella, C., Campanella, A., De Falco, L., Boschetto, L., Merlini, R., Silvestri, L., Levi, S., and Iolascon, A. (2007). The human counterpart of zebra fish shiraz shows sideroblastic like microcytic anemia and iron overload. Blood *110*, 1353 1358.

Campuzano, V., Montermini, L., Molto, M.D., Pianese, L., Cossee, M., Caval canti, F., Monros, E., Rodius, F., Duclos, F., Monticelli, A., et al. (1996). Frie dreich's ataxia: autosomal recessive disease caused by an intronic GAA triplet repeat expansion. Science *271*, 1423 1427.

Dittmer, P.J., Miranda, J.G., Gorski, J.A., and Palmer, A.E. (2009). Genetically encoded sensors to elucidate spatial distribution of cellular zinc. J. Biol. Chem. *284*, 16289 16297.

Djaman, O., Outten, F.W., and Imlay, J.A. (2004). Repair of oxidized iron sulfur clusters in Escherichia coli. J. Biol. Chem. *279*, 44590 44599.

Domaille, D.W., Que, E.L., and Chang, C.J. (2008). Synthetic fluorescent sensors for studying the cell biology of metals. Nat. Chem. Biol. *4*, 168 175.

Finsterer, J. (2008). Leigh and Leigh like syndrome in children and adults. Pe diatr. Neurol. *39*, 223 235.

Fosset, C., Chauveau, M.J., Guillon, B., Canal, F., Drapier, J.C., and Bouton, C. (2006). RNA silencing of mitochondrial m Nfs1 reduces Fe S enzyme activity both in mitochondria and cytosol of mammalian cells. J. Biol. Chem. *281*, 25398 25406.

Gladyshev, V.N., Liu, A., Novoselov, S.V., Krysan, K., Sun, Q.A., Kryukov, V.M., Kryukov, G.V., and Lou, M.F. (2001). Identification and characterization of a new mammalian glutaredoxin (thioltransferase), Grx2. J. Biol. Chem. *276*, 30374 30380.

Greeson, J.N., Organ, L.E., Pereira, F.A., and Raphael, R.M. (2006). Assess ment of prestin self association using fluorescence resonance energy transfer. Brain Res. *1091*, 140 150.

Hoff, K.G., Silberg, J.J., and Vickery, L.E. (2000). Interaction of the iron sulfur cluster assembly protein IscU with the Hsc66/Hsc20 molecular chaperone system of Escherichia coli. Proc. Natl. Acad. Sci. USA *97*, 7790 7795.

Hoff, K.G., Goodlitt, R., Li, R., Smolke, C.D., and Silberg, J.J. (2009). Fluores cence detection of a protein bound 2Fe2S cluster. ChemBioChem *10*, 667 670.

Horton, R.M., Hunt, H.D., Ho, S.N., Pullen, J.K., and Pease, L.R. (1989). Engi neering hybrid genes without the use of restriction enzymes: gene splicing by overlap extension. Gene *77*, 61 68.

Hu, C.D., and Kerppola, T.K. (2003). Simultaneous visualization of multiple protein interactions in living cells using multicolor fluorescence complementa tion analysis. Nat. Biotechnol. *21*, 539 545.

Hudemann, C., Lonn, M.E., Godoy, J.R., Zahedi Avval, F., Capani, F., Holmg ren, A., and Lillig, C.H. (2009). Identification, expression pattern, and charac terization of mouse glutaredoxin 2 isoforms. Antioxid. Redox Signal. *11*, 1 14.

Huttemann, M., Schmidt, T.R., and Grossman, L.I. (2003). A third isoform of cytochrome c oxidase subunit VIII is present in mammals. Gene *312*, 95 102.

Iwema, T., Picciocchi, A., Traore, D.A., Ferrer, J.L., Chauvat, F., and Jacqua met, L. (2009). Structural basis for delivery of the intact [Fe2S2] cluster by monothiol glutaredoxin. Biochemistry *48*, 6041 6043.

Johansson, C., Kavanagh, K.L., Gileadi, O., and Oppermann, U. (2007). Reversible sequestration of active site cysteines in a 2Fe 2S bridged dimer provides a mechanism for glutaredoxin 2 regulation in human mitochondria. J. Biol. Chem. *282*, 3077 3082.

Kerppola, T.K. (2006). Visualization of molecular interactions by fluorescence complementation. Nat. Rev. Mol. Cell Biol. *7*, 449 456.

Lee, D.W., Kaur, D., Chinta, S.J., Rajagopalan, S., and Anderson, J.K. (2009). A disruption in iron sulfur center biogenesis via inhibition of mitochondrial dithiol glutaredoxin 2 may contribute to mitochondrial and cellular iron dysregulation in mammalian glutathione depleted dopaminergic cells: implications for Parkinson's disease. Antioxid. Redox Signal. *11*. in press.

Li, H., Mapolelo, D.T., Dingra, N.N., Naik, S.G., Lees, N.S., Hoffman, B.M., Riggs Gelasco, B.J., Huynh, B.H., Johnson, M.K., and Outten, C.E. (2009). The yeast iron regulatory proteins Grx3/4 and Fra2 form heterodimeric complexes containing a [2Fe 2S] cluster with cysteinyl and histidyl ligation. Biochemistry *8*, 9569 9581.

Lill, R. (2009). Function and biogenesis of iron sulphur proteins. Nature *460*, 831 838.

Lill, R., and Muhlenhoff, U. (2008). Maturation of iron sulfur proteins in eukary otes: mechanisms, connected processes, and diseases. Annu. Rev. Biochem. *77*, 669 700.

Lillig, C.H., Berndt, C., Vergnolle, O., Lonn, M.E., Hudemann, C., Bill, E., and Holmgren, A. (2005). Characterization of human glutaredoxin 2 as iron sulfur protein: a possible role as redox sensor. Proc. Natl. Acad. Sci. USA *102*, 8168 8173.

Lillig, C.H., Berndt, C., and Holmgren, A. (2008). Glutaredoxin systems. Biochim. Biophys. Acta *1780*, 1304 1317.

Livak, K.J., and Schmittgen, T.D. (2001). Analysis of relative gene expression data using real time quantitative PCR and the 2(Delta Delta C(T)) Method. Methods *25*, 402 408.

Lonn, M.E., Hudemann, C., Berndt, C., Cherkasov, V., Capani, F., Holmgren, A., and Lillig, C.H. (2008). Expression pattern of human glutaredoxin 2 iso forms: identification and characterization of two testis/cancer cell specific isoforms. Antioxid. Redox Signal. *10*, 547 557.

Lundberg, M., Johansson, C., Chandra, J., Enoksson, M., Jacobsson, G., Ljung, J., Johansson, M., and Holmgren, A. (2001). Cloning and expression of a novel human glutaredoxin (Grx2) with mitochondrial and nuclear isoforms. J. Biol. Chem. *276*, 26269–26275.

Magliery, T.J., Wilson, C.G., Pan, W., Mishler, D., Ghosh, I., Hamilton, A.D., and Regan, L. (2005). Detecting protein-protein interactions with a green fluorescent protein fragment reassembly trap: scope and mechanism. J. Am. Chem. Soc. *127*, 146–157.

Mochel, F., Knight, M.A., Tong, W.H., Hernandez, D., Ayyad, K., Taivassalo, T., Andersen, P.M., Singleton, A., Rouault, T.A., Fischbeck, K.H., and Haller, R.G. (2008). Splice mutation in the iron-sulfur cluster scaffold protein ISCU causes myopathy with exercise intolerance. Am. J. Hum. Genet. *82*, 652–660.

Morell, M., Czihal, P., Hoffmann, R., Otvos, L., Aviles, F.X., and Ventura, S. (2008). Monitoring the interference of protein-protein interactions in vivo by bimolecular fluorescence complementation: the DnaK case. Proteomics *8*, 3433–3442.

Muhlenhoff, U., Richhardt, N., Gerber, J., and Lill, R. (2002). Characterization of iron-sulfur protein assembly in isolated mitochondria. A requirement for ATP, NADH, and reduced iron. J. Biol. Chem. *277*, 29810–29816.

Muhlenhoff, U., Gerber, J., Richhardt, N., and Lill, R. (2003). Components involved in assembly and dislocation of iron-sulfur clusters on the scaffold protein Isu1p. EMBO J. *22*, 4815–4825.

Nagai, T., Ibata, K., Park, E.S., Kubota, M., Mikoshiba, K., and Miyawaki, A. (2002). A variant of yellow fluorescent protein with fast and efficient maturation for cell-biological applications. Nat. Biotechnol. *20*, 87–90.

O'Shea, E.K., Klemm, J.D., Kim, P.S., and Alber, T. (1991). X-ray structure of the GCN4 leucine zipper, a two-stranded, parallel coiled coil. Science *254*, 539–544.

Pelletier, J.N., Campbell-Valois, F.X., and Michnick, S.W. (1998). Oligomerization domain-directed reassembly of active dihydrofolate reductase from rationally designed fragments. Proc. Natl. Acad. Sci. USA *95*, 12141–12146.

Pierik, A.J., Netz, D.J., and Lill, R. (2009). Analysis of iron-sulfur protein maturation in eukaryotes. Nat. Protoc. *4*, 753–766.

Raulfs, E.C., O'Carroll, I.P., Dos Santos, P.C., Unciuleac, M.C., and Dean, D.R. (2008). In vivo iron-sulfur cluster formation. Proc. Natl. Acad. Sci. USA *105*, 8591–8596.

Rees, D.C., and Howard, J.B. (2003). The interface between the biological and inorganic worlds: iron-sulfur metalloclusters. Science *300*, 929–931.

Song, D., and Lee, F.S. (2008). A role for IOP1 in mammalian cytosolic iron-sulfur protein biogenesis. J. Biol. Chem. *283*, 9231–9238.

Stefan, E., Aquin, S., Berger, N., Landry, C.R., Nyfeler, B., Bouvier, M., and Michnick, S.W. (2007). Quantification of dynamic protein complexes using Renilla luciferase fragment complementation applied to protein kinase A activities in vivo. Proc. Natl. Acad. Sci. USA *104*, 16916–16921.

Tong, W.H., and Rouault, T.A. (2006). Functions of mitochondrial ISCU and cytosolic ISCU in mammalian iron-sulfur cluster biogenesis and iron homeostasis. Cell Metab. *3*, 199–210.

Veatch, J.R., McMurray, M.A., Nelson, Z.W., and Gottschling, D.E. (2009). Mitochondrial dysfunction leads to nuclear genome instability via an iron-sulfur cluster defect. Cell *137*, 1247–1258.

Whitnall, M., Rahmanto, Y.S., Sutak, R., Xu, X., Becker, E.M., Mikhael, M.R., Ponka, P., and Richardson, D.R. (2008). The MCK mouse heart model of Friedreich's ataxia: Alterations in iron-regulated proteins and cardiac hypertrophy are limited by iron chelation. Proc. Natl. Acad. Sci. USA *105*, 9757–9762.

Yang, J., Naik, S.G., Ortillo, D.O., Garcia-Serres, R., Li, M., Broderick, W.E., Huynh, B.H., and Broderick, J.B. (2009). The iron-sulfur cluster of pyruvate formate-lyase activating enzyme in whole cells: Cluster interconversion and a valence-localized [4Fe-4S]2+ state. Biochemistry *8*, 9234–9241.

